HIGH-SPEED SCHLIEREN IMAGING AND POST-PROCESSING FOR INVESTIGATION OF FLAME PROPAGATION WITHIN DROPLET-VAPOUR-AIR FUEL MIXTURES

(Date received: 21.5.2007)

Shaharin Anwar Sulaiman[1] and Malcolm Lawes[2]

[1] Mechanical Engineering Programme, Universiti Teknologi Petronas, 31750 Tronoh, Perak

[2]School of Mechanical Engineering, University of Leeds, Leeds LS2 9JT, United Kingdom

Email: shaharin@petronas.com.my

ABSTRACT

Studies in practical spray combustion systems are complex due to the presence of various dependent parameters such as turbulence and inhomogeneity of physical properties of the reactants. Therefore, fundamental aerosol combustion studies are required so that practical combustion of aerosols and sprays can be understood. To another extent, data on laminar burning velocities, which is well known to play an important role in turbulent combustion, is still very scarce particularly for droplet-vapour-air mixtures. Previous researches demonstrated that the presence of liquid droplets in the combustion of aerosol mixtures could influence flame instabilities. These instabilities, which are characterized by cellular and wrinkling flame structures, promote a faster burning rate. Nevertheless, due to the technique and condition of the imaging system available in the past, the critical properties related to flame instabilities, for instance the point of the onset of cellularity, were unclear. In this paper, applications of high-speed schlieren imaging and a digital image processing techniques are presented and discussed. It is shown that the use of a digital camera coupled with an accurate synchronisation system produces better image quality of the flames as compared to the previous techniques. The improved image processing technique is shown to be potential in reducing the processing time and errors.

Keywords: *Aerosol, Instabilities, Laminar Flames, Optical Diagnostics, Sprays*

1. INTRODUCTION

The combustion of fuel sprays is of practical importance in diesel and spark ignition engines, furnaces and hazardous environments. However, studies in practical systems are unsuitable for this purpose, due to the multiplicity of dependent parameters. In a Direct Injection Spark Ignition (DISI) engines, for example, the flame propagation rate in the two-phase-environment must be analysed in isolation from the complex processes of fuel injection and mixing, often within a turbulent flow field. At present, the interaction of these processes does not allow for adequate mathematical modelling.

Theoretical [1, 2] and experimental [3-5] evidences suggest that, flame propagation through vapour clouds, under certain circumstances, is higher than that in a fully vaporised homogeneous mixture. Even though this may be advantageous in giving more rapid burning, its effects on emissions are uncertain. Conversely, it is a serious disadvantage in the hazard context. Although most practical combustion takes place under turbulent conditions, it is well established that the laminar burning rate plays an important role in turbulent combustion [6]. For instance, the fuel's burning velocity affects the burn rate in a spark-ignition engine and therefore its efficiency [7]. At present, information on laminar burning velocity for fuel sprays and for gas-liquid co-burning [8-11] is sparse, even for gaseous mixtures at conditions pertaining to engines, which range from sub-atmospheric to high pressure and temperature. As a consequence, there is little experimental data (of a fundamental) nature that clearly demonstrates the similarities and differences in burning rate, either laminar or turbulent, between single and two phase combustion.

The techniques for the measurements of laminar burning velocity were widely reviewed by Andrews and Bradley [12]. A method that is based on the rate of disappearance of cold, unburned gas is determined from photographic observation of the cold flame front. Among the optical methods suitable for this is the high-speed schlieren photography, a visualisation technique that relies on the difference in fluid densities (and thus refractive index) in regions of transparent medium. This technique is simple, inexpensive and satisfactorily accurate. Previous applications of this technique in flame propagation studies [13-15], made use of a rotating drum camera and film to record flame images at high speed. However this type of image recording system is difficult to synchronise and requires a long post-processing time. In the present work, the burning rate and instabilities of spherically propagating flame of aerosol mixtures were studied. The applications of high-speed schlieren imaging and a digital image processing techniques for the study of such flames are presented and discussed. A digital camera, which was coupled with an accurate synchronisation system, was used in order to improve the image quality and accuracy of the explosion timing. In addition, a digital post-processing method for analysing the propagation rate of aerosol flames was introduced to obtain quicker and better results, as compared to the previous technique.

2. SCHLIEREN OBSERVATION TECHNIQUE

The schlieren observation technique is generated from a German word denoting optical inhomogeneity in a region or medium that is transparent to the naked eye. This causes refraction of light which can be displayed on a screen and used as a source of information on the disturbance [16]. In the context of the present work, the schlieren image of the inhomogeneity recorded was the refractive index gradient, resulting from density gradients in the reaction zone

of a flame. Further details of the principle of operation applied to combustion can be found in various literatures, for instance in [17].

The use of schlieren technique in the flame propagation studies is primarily intended to quantify the burning rates. It is also used to observe the flame's surface structure, which is associated to the burning velocity; for instance a cellular flame has a greater surface area and hence experiences higher burning rate than that of a smooth flame. Examples of the application of this technique in flame propagation studies on gaseous mixtures are available in [13, 14]. For spray combustion, these are found in [10, 11, 15, 18-21]. However, rotating drum cameras with film were used in the past to record flame images at high speed (typically between 300 and 10,000 frames per second). This method was quite difficult to perform because the optical settings involved some trial-and-error approach. In addition the films used in this technique required processing in order to obtain negatives; this took several hours after each experiment run.

One other disadvantage suffered by the previous works was the inaccuracy in synchronisation between equipment. This was another critical factor because the flame propagation period was very fast, typically within 50 ms.

3. LAMINAR BURNING RATES

For the observation of spherically propagating flame of gaseous mixtures, the schlieren technique was much earlier used by Hundy [22] for the measurements of flame speeds in order to deduce important properties such as burning velocities and flame stretch. With this technique, images of flame front were captured for the measurements of cold front radii defined as the isotherm of 5 K above the reactant temperature [23]. The direct measurement of flame front radius, *r*, enables calculations of the stretched laminar flame speed, S_n, given by:

$$S_n = \frac{dr}{dt} \tag{1}$$

Flame sheets are subject to the effects of flow strain rate and flame curvature, which stretch the flame. This stretch can increase or decrease the burning velocity [24, 25]. The rate of flame stretch, α, is defined as the time derivative of the area, A, of an infinitesimal element divided by the area, and for a spherical flame, this becomes:

$$\alpha = \frac{1}{A}\frac{dA}{dt} = \frac{2}{r}\frac{dr}{dt} = \frac{2}{r}S_n \tag{2}$$

Obviously Equation (2) shows that α is inversely proportional with *r*. The gradient of the best straight line-fit for the plot of S_n against α yields the burned gas Markstein length, L_b [26], which expresses the influence of stretch on the flame speed by:

$$S_n = S_n - L_b\alpha \tag{3}$$

where S_s is the unstretched flame speed, defined as the value of S_n at $\alpha = 0$ (at a very large flame radius) in the plot of S_n against α. The unstretched laminar burning velocity u_l, is deduced from S_s since, for approximately constant pressure flame propagation, u_l and S_s are related by:

$$u_l = S_s\frac{\rho_b}{\rho_u} \tag{4}$$

where ρ_b and ρ_u are burnt and unburnt densities of the gaseous mixture. Extended calculations of higher level properties of flame propagation and their significances are presented in the references and are not intended for discussion in this paper.

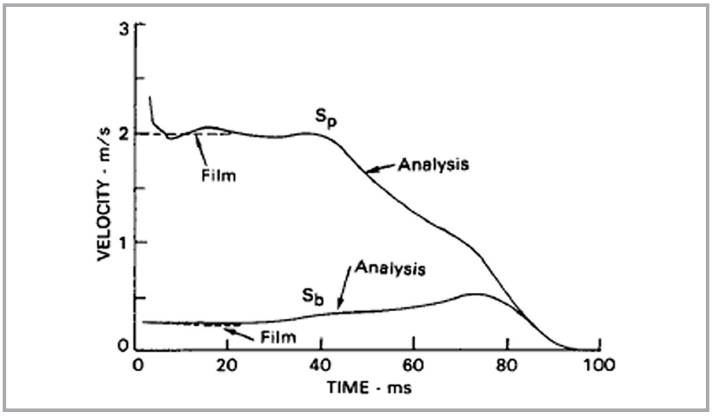

Figure 1: Flame speed as a function of time for a mixture of propane-air at ø = 1.0, reproduced from [29]

An alternative to the schlieren technique, for the investigation of burning velocity, is the pressure-time method. Here the flame speeds are computed from measured pressure-time data using a two-zone thermodynamic combustion model, as described by Groff [29]. This method uses t-ime derivatives of experimental pressure data using a numerical method package. Figure 1 shows a typical comparison of flame speeds of a spherically propagating flame in a constant volume vessel between the schlieren and pressure-time methods [29]. In general the results show good agreement between the two methods. It is also shown that at the initial stage of the flame development; that is when the flame radius is small, the schlieren method gives more reliable results than that of the pressure-time method. On the other hand it is worth noting that the schlieren observation technique is limited to the field of view of the optical and image recording system, whereas the pressure-time method can measure up to a greater flame radius.

4. EXPERIMENTAL SETUP AND TECHNIQUES

A. COMBUSTION APPARATUS

The combustion apparatus is shown schematically, in Figure 2. Full descriptions of the system and aerosol generation technique were presented elsewhere in [30]. The combustion vessel (CV) was a cylindrical vessel with the internal diameter and length equal to 305 mm. Optical access windows of 150 mm diameter were provided on both end plates for characterisation of aerosol and schlieren photography of flame propagation. Four fans, driven by electric motors, adjacent to the wall of the vessel, were used to mix the reactants during preparation. Two electrical heaters were attached to the wall of the vessel to preheat the vessel and mixture to 303 K.

B. MIXTURE PREPARATION

Aerosol mixtures were prepared by a condensation technique based on the Wilson cloud principle [31] to generate well defined, narrowly-dispersed droplet suspensions in-situ by controlled expansion of a gaseous iso-octane-air mixture from the combustion vessel into the expansion vessel, which was pre-evacuated to less than 1 kPa. This caused a reduction in mixture pressure and temperature, which took it into the wet regime and caused droplets to be formed. Details of the characterization of the mixture droplets are reported in [30]. The droplet arithmetic mean diameter, D10, which varied with time during expansion, was measured in-situ, without combustion, using a Phase Doppler Anemometer (PDA) system. Since the expansion took place over a period of several seconds while combustion took place over less than 80 ms, far field values of D10 were assumed to be constant during combustion.

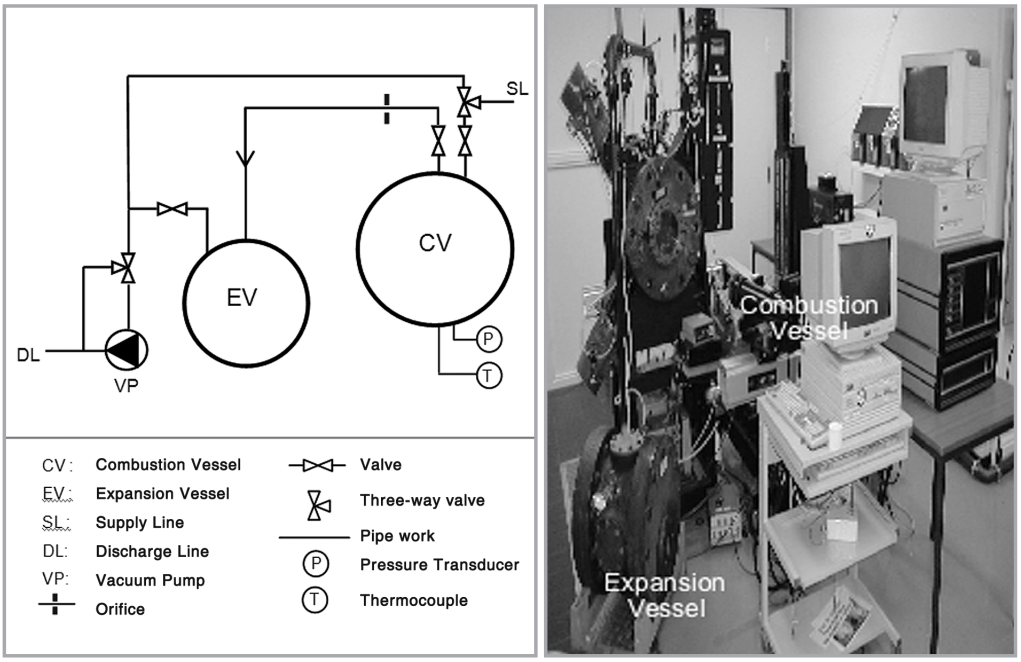

Figure 2: Experiment setup: (a) Schematic of aerosol combustion apparatus, and (b) picture of experiment rig

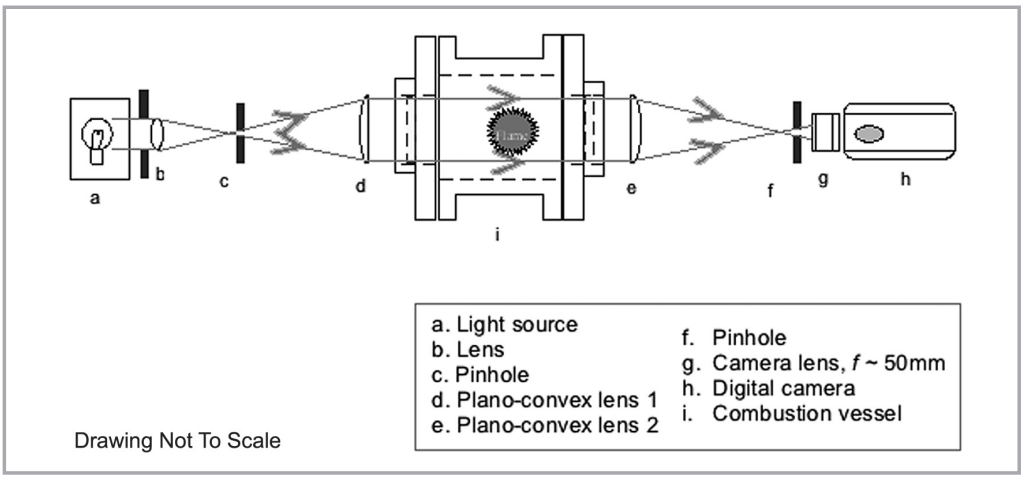

Figure 3: Schematic of camera and optical settings for schlieren imaging

C. CAMERA AND OPTICAL SETTINGS

The aerosol mixture was ignited at the centre of the combustion vessel by an electric spark of about 500 mJ. The flame front was monitored with a high speed digital camera at a rate of 1000 frames per second through the vessel's windows. Figure 3 shows the optical setting for the schlieren imaging system used in the present work. For the main experiments, the light, which was generated from a halogen lamp, was expanded to a diameter of approximately 150 mm by a biconvex lens, as shown in Figure 3. The light was then collimated by a 150 mm diameter plano-convex lens (f = 1000 mm) before passing through the two optical windows of the explosion vessel. Upon passing through the fluid media in the vessel, some part of the light would be deflected due to the density gradient resulted by the flame temperature. The deflected light was focused by a second identical plano-convex lens onto a pinhole, beyond which the schlieren image of the flame could be projected on a perpendicular surface. The schlieren image was observed and recorded using a Phantom (Vision Research Inc.) high speed digital camera, which was operated by Phantom software in a computer. The camera generated monochrome 512 by 512 pixel images with sensitivity equivalent to 1600 ASA (American Standard Association) in a computer. At full resolution it was capable to capture the flame image at 1 ms interval per frame.

The post-triggering feature available in the camera software enabled recording of images prior to ignition to overcome time delays related to electronic signal between the equipment. The exposure time used in the photography was normally 17 μs but in the event of very dense aerosol the setting was changed to 28 μs. To scale the flame, the image of a transparent reference grid was placed on the optical access prior to the experiment.

D. SYNCHRONISATION

Figure 4 shows the schematic of the synchronisation between the start of expansion and the initiations of both the image recording (high speed camera) and the spark ignition. The safety valve switch (SVS), which comprised a sensor and circuit, protect the pressure transducer during combustion. When the expansion valve, which linked the two vessels, was opened, it activated the principal trigger switch (PTS) to send a signal to start an Omron H8GN countdown timer. The delay setting for the timer was between 0 and 3.5 s, depending on the aerosol characterization profile described in Section 4B. The signal from the timer was transformed by the signal converter into break (OFF) and make (ON) signals for the camera and ignition systems, respectively. The signal for the camera trigger was converted into a light pulse by the opto-isolator depicted in Figure 4. This isolated the camera trigger system from signal interference generated by the ignition unit.

5. IMAGE POST-PROCESSING

Previously [20, 21, 32], the post-processing of the flame images was done manually, by obtaining three diameter measurements from every single flame image. The locations of measurement were at the cross-sections perpendicular to the electrode, and at an angle 45o relative to the electrode holder [33]. In the present work, the processing technique for the schlieren images of aerosol flames was similar to that presented by Ormsby [34] in his study using gaseous flames. A typical flame movie consisted series of between 30 and 80 frames of images at an interval of one millisecond. The first image would be the one just before the start of ignition, and the last being the one at which the flame front was observed to reach the circular boundary of the access windows.

Figure 5 shows the flow chart for the tasks involved in the image post-processing. The purpose of the image processing was

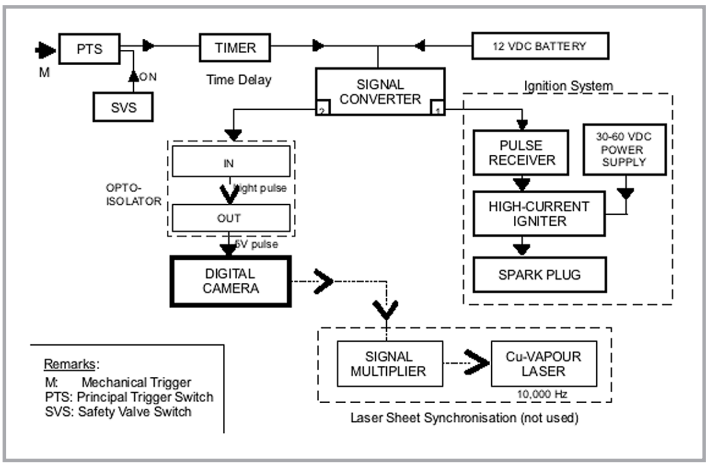

Figure 4: Schematic for trigger control of ignition and camera systems

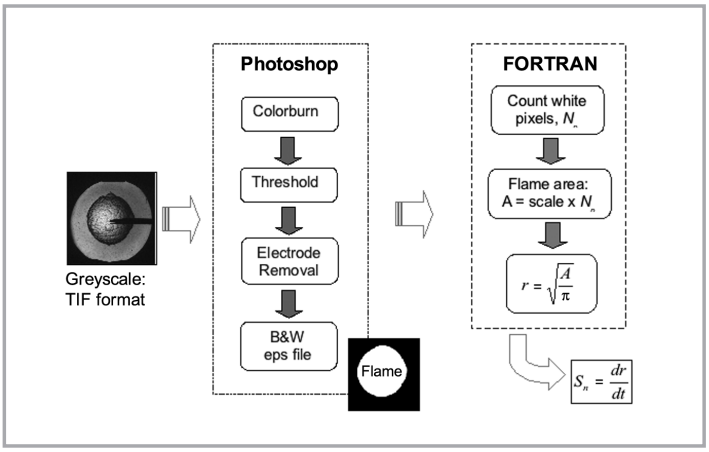

Figure 5: Flow chart for post-processing

to convert the original image into a simpler picture system, which contained only pure white (flame) and pure black (background) colours, using Photoshop software so that the area within the circular shape of the flame can be quantified. Any other colours within the area of the flame must be converted into white, and those outside the flame shall be completely blackened. The number of white pixels, which represented the flame frontal area, was counted using a FORTRAN program. The actual frontal area of the flame was calculated from a known scale, derived from a transparent grid of 10 mm × 10 mm that was attached to the window of the vessel. With the availability of the true area of the white object, the radius of the flame was determined using the equation for a circle area, as indicated in Figure 5.

The Photoshop part of the processing of the flame images, as depicted in Figure 5, involved both manual and automatic tasks. Each picture, which was of 512 pixels by 512 pixels, was originally in a greyscale Tagged Image File (TIF) format. Each of the grey images had a bimodal threshold histogram, in which there were two peaks, one for the foreground and another for the background. In this stage the image background was blackened while the flame body was whitened, hence the threshold histogram would be of single peak. In the Adobe Photoshop software, the background of the flame ball was first removed or blackened by using the colorburn layer blending command. Figure 6 shows the step involved in the colorburn process. An image without flame, captured before ignition (Figure 6a), was pasted onto an inverted image of flame (Figure 6b). The result of the colorburn blending is shown in Figure 6c, in which the flame background has been blackened thus providing a circular area that defined the flame frontal area. Adjustment on the image threshold resulted in a distinct white area (flame) on the black background; this is shown in Figure 7a. However, the spark electrode holder displayed as a horizontal object located on the right hand side of the flame caused a discontinuity on the white area and thus must be removed.

Figure 7 shows the step involved in removing the spark electrode holder. This was done manually by carefully drawing a white line crossing the electrode holder as shown Figure 7a. Since this line is short relative to the perimeter of the flame, the resulting error is assumed negligible. With a full continuous flame boundary, as shown in Figure 7b, the flame frontal area was filled with white colour, to remove the black area within the central region, using the fill command in the Adobe Photoshop software. The result is depicted in Figure 7c. The image was finally saved as an encapsulated postscript (eps) ASCII format file so that it could be recognised and read as input by a computer programme. Considering the large number of pictures (30 to 80) to be processed for each flame movie, it could take some time to complete the task if the whole process was done one by one. However with an automation feature available in the software, many of the tasks could be repeated automatically and thus faster than those done manually.

A FORTRAN program was developed earlier in gaseous studies [33] to read the encapsulated postscript (eps) file as a data input and to calculate the number of white pixels in each image,

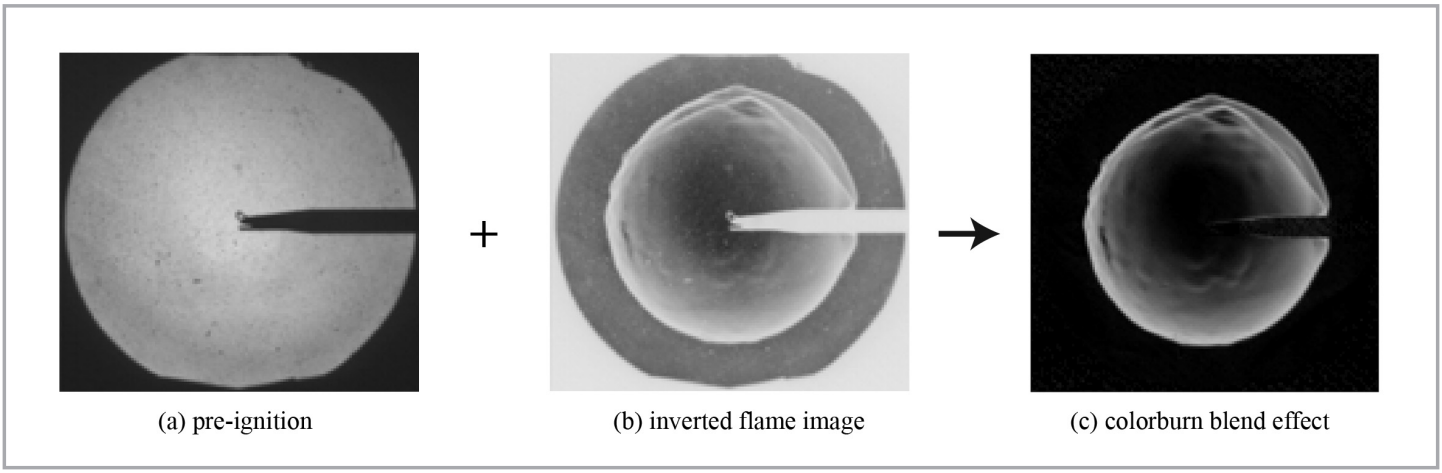

Figure 6: Background blackening of schlieren image of flame by colorburn method

Figure 7: Stage 2 of image post-processing for removal of electrode holder and definition of frontal flame surface

which represented the frontal area of the flame. It must be noted that the image in the generated eps file consisted of black and white colours only. The greyscale has 256 levels of color intensity levels ranging between 0 (pure black) and 255 (pure white). This file can also be read in term of ASCII code (numbers), which is viewable in text software such as Notepad. The FORTRAN program counted the number of white pixels (level 255) by reading from the ASCII code in the eps file. The flame radius was calculated by the program as the radius of a circle that has the same area (white pixels) of the flame. From time and distance measurements, flame radii against time data were calculated using the equation for a circle area as depicted in Figure 5. These were further analysed in commercial spreadsheet software to derive the flame speed and laminar burning velocity.

6. RESULTS
A. FLAME OBSERVATIONS

Shown in Figure 8 are sequences of typical flames of stoichiometric aerosols with droplet sizes of (a) 5 μm and (b) 10 μm. Both flames are compared at similar radii as indicated in Figure 8. Also shown in each photograph is the time from ignition. The mixtures were initially at pressures between 172 and 185 kPa, and temperatures between 278 and 281 K. It must be noted that the small difference in the pressures and temperatures between the conditions in the two flames has been shown, for gaseous flames, to have little effect on the flame structure [23]. Hence, it is assumed that the difference in the structure is entirely due to the effects of droplets.

In Figure 8a, with the smaller droplets, the flame was initially smooth, without cells. The long cracks on the surface of the flame were originated by the perturbation from the spark electrode, and these changed very little throughout flame propagation. The first sign of change in the smooth flame surface structure in Figure 8a was observed at a radius of approximately 40 mm, as denoted by the shallow cells. Throughout the flame propagation, the cells, which were of the order of several millimetres in diameters, became more pronounced. The cell boundaries appear to be associated with valleys between wrinkles. At a radius of 60 mm the flame surface displayed scattered and increasing number of cells. The flame became fully cellular after an extended period of time at which the flame propagated beyond the radius of vessel windows. The flame structure for the aerosol with larger droplet diameters was similar to those for 5 μm except that the cells developed more rapidly. At a flame radius of 10 mm, both flames in Figure 8 were smooth. However, for the 10 μm droplets full cellularity was obtained at

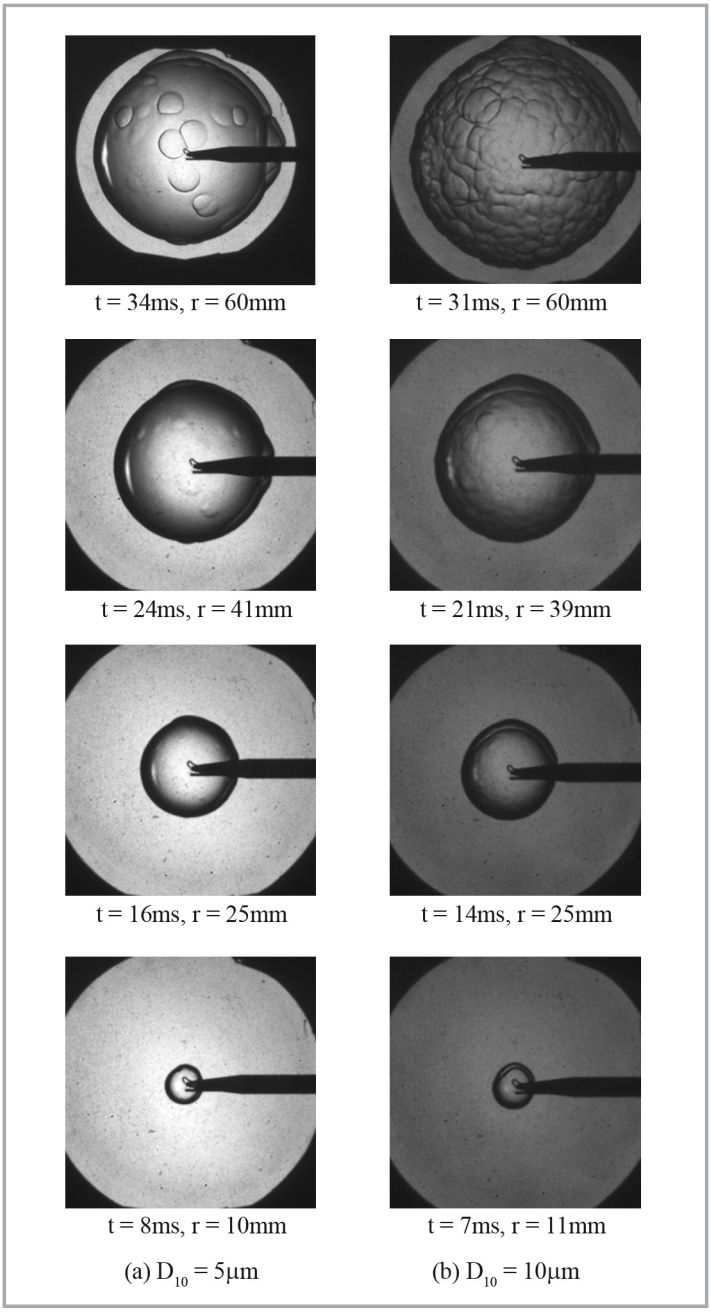

Figure 8: Sequences of schlieren images of flames within stoichiometric (ϕ_{ov} = 1.0) aerosols at (a) P = 185 kPa, T = 281 K and D_{10} = 5 μm, and (b) P = 172 kPa, T = 278 K and D_{10} = 10 μm

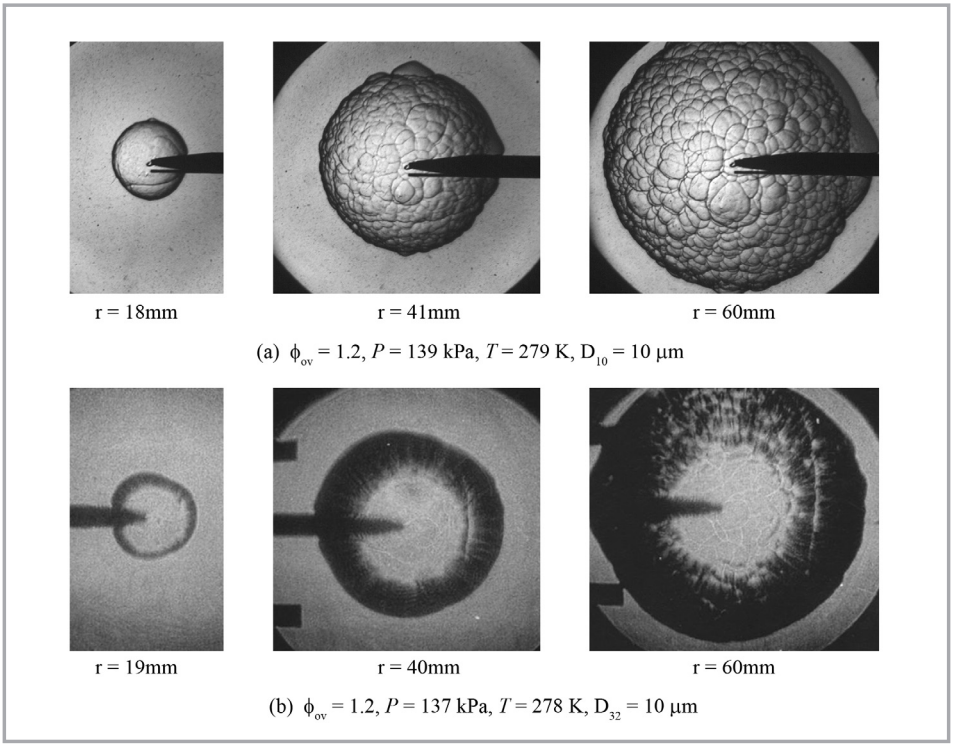

Figure 9: Comparison of flame structures of iso-octane-air aerosol at similar mixture conditions, obtained by different imaging recording systems; (a) with digital camera and (b) with drum camera [15]

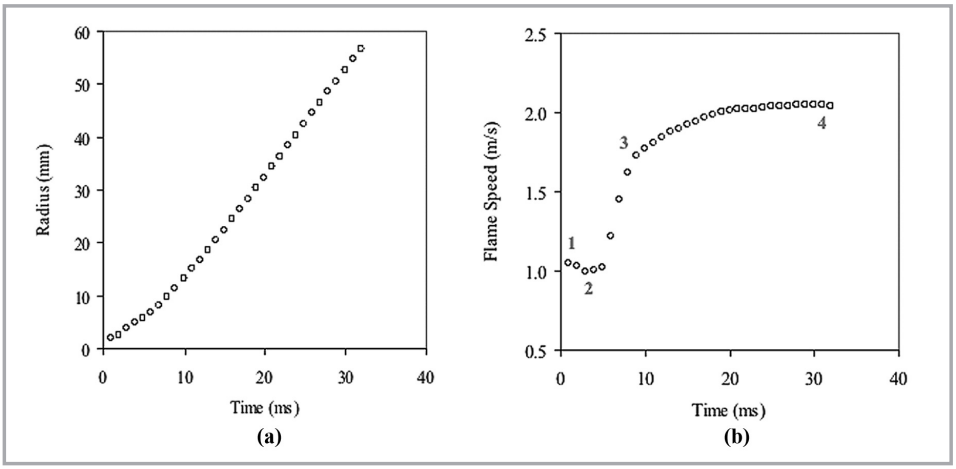

Figure 10: Typical variations of (a) radius and (b) flame speed, with time from start of ignition for a laminar aerosol flame at ϕ_{ov} = 1.0, D10 = 8 μm, P = 134 kPa and T = 277 K

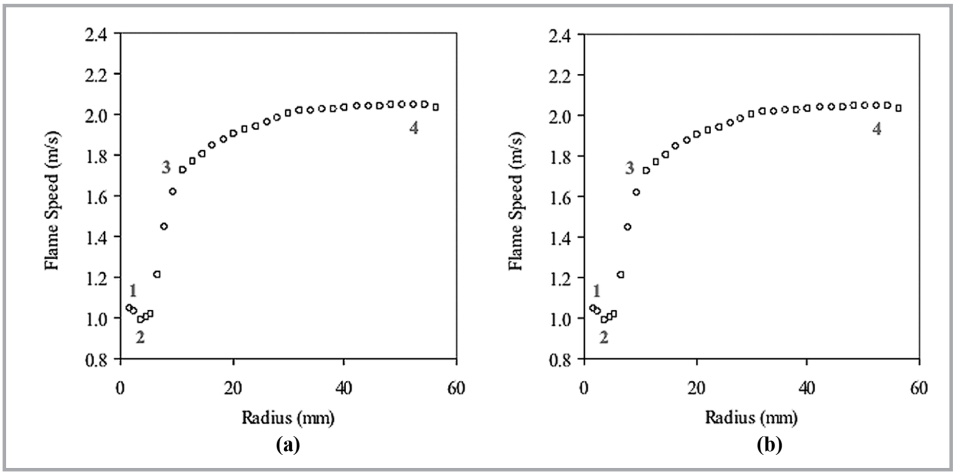

Figure 11: Typical variations of flame speed with (a) radius and (b) flame stretch for aerosol described for Figure 10

about 52 mm, which was earlier than that for the 5 μm droplets.

In the present work a high-speed digital camera was used for studies of laminar flames within aerosols, whereas in previous studies [15, 20, 21], a drum camera was used for similar purposes. The differences between the images produced by the two cameras are compared here. Shown in Figure 9a are sequences of typical flame photographs obtained using the high-speed digital camera in the present work for aerosols at ϕ_{ov} = 1.2, P = 137 kPa, T = 278 K and D_{10} = 10 μm. In Figure 9b the typical flame images produced by the drum camera at similar conditions in the same explosion vessel are shown.

It is shown that the images in Figure 9a, obtained with the digital camera, are considerably sharper and clearer than those obtained with the drum camera. In particular the cells are more clearly defined, making studies of the onset of instabilities much more accurate than was previously possible. This is particularly well illustrated by the images at about 40 mm in diameter. Here, any cellularity in the image from the drum camera is unclear, yet the digital camera revealed that cellularity was well developed. For example, Atzler [15] reported that cellularity started in Figure 9b at a flame radius of 50 mm. However, in Figure 9a the same effect was shown to occur at a flame radius of approximately 18 mm. These radii could be used to determine the crticial Peclet number, Pecr [25]. Thus it is suggested from Figure 9 that the value of Pecr in the work of Atzler was probably over estimated.

B. COMPARISON OF QUANTITATIVE BURNING PROPERTIES

Shown in Figure 10 are typical variations of flame radius and flame speed with time, respectively, for a laminar flame of an iso-octane-air aerosol at ϕ_{ov} = 1.0, D_{10} = 8 μm, P = 134 kPa and T = 277 K. The radius data points shown in Figure 10a were obtained from the image processing procedure as illustrated in Figure 5. The flame speed in Figure 10b was obtained using Equation (1). The results in Figure 10 are usually presented in terms of flame speed versus radius and flame speed versus flame stretch, as shown in Figures 11a and 11b, respectively. In Figure 11b, the flame stretch was obtained from Equation (2) and the point of ignition

is located to the right, at a high stretch rate, and flame propagation is from right to left.

Figures 10 and 11 clearly exhibit regimes of flame development [35], as indicated by points (1) to (4). The ignition started at point (1) where the flame speed was the result of active radicals provided by the spark energy. However, high stretch rates caused the flame speed to decrease rapidly when the thermal energy of the spark was dissipated into the reactant and before normal flame chemistry developed. At point (2), a propagating flame probably was not yet established. Between points (2) and (3), spark plasma dynamics and flame stretch were operative in a regime of spark assisted flame propagation. Between points (3) and (4) flame speed increased as the rate of stretch reduced. All flames in the present work exhibited these trends. However, the spark affected period, between points (1) and (3), was not important to the present work since it was shown elsewhere [23] that the flame propagation after this period would be independent of the spark energy. It is evident from Figure 11a that flame is fully developed only at radii bigger than about 16 mm. Bradley *et al.* [23], who studied gaseous flames at temperatures higher than 358 K, suggested that flames were not fully developed for the determination of burning rates at radii less than 10 mm. The late development of flames in the present research compared to previous gaseous flame studies could be associated with the low temperature ($\leq$ 303 K) at ignition used in the present work.

In Figure 11b, the line indicates the unstretched flame speed, S_s, which is derived by a linear extrapolation to zero stretch. The laminar burning velocity, u_l, can be calculated from S_s using Equation (4). The negative of the gradient of the extrapolation is the burnt gas Markstein length, L_b, which is expressed in Equation (3). A positive value of L_b, that is increasing flame speed with decreasing stretch rate, indicates a flame with little tendency to instabilities, and conversely, a mixture with negative L_b tends to develop instabilities much quicker [25].

7. CONCLUSION

Applications of high-speed schlieren imaging and a digital image processing techniques are presented in this paper. It is suggested that the use of a digital camera coupled with an accurate synchronisation system produces good image quality of the flames. A comparison between the present results and those obtained using a drum camera shows significant improvement, such that the inception and size of cells on the flame surface are more clearly defined, which enabled clear distinction between cellular and smooth flame surface in order to determine flame instabilities. In addition, the digitised image processing technique is shown to be more effective as the processing time has been reduced and human-related errors been minimised. Thus the technique presented here is proven useful and would be recommended for use in future experiments involving aerosol flames. ■

GREEK SYMBOLS

α	flame stretch, s^{-1}
ϕ_{ov}	overall equivalence ratio (two-phase mixture)
ρ_b	density of burned gaseous, kg/m^3
ρ_u	density of unburned mixtures, kg/m^3

NOMENCLATURE

A	flame area, m^2
D_{10}	arithmetic droplet mean diameter, μm
L_b	Markstein length, mm
P	pressure, kPa
r	flame radius, mm
S_n	stretched laminar flame speed, m/s
S_s	unstretched laminar flame speed, m/s
T	temperature, K
t	time, ms
u_l	laminar burning velocity, m/s

REFERENCES

[1] J. B. Greenberg, "Propagation and Extinction of an Unsteady Spherical Spray Flame Front," Combust. Theory Modelling, vol. 7, pp. 163-174, 2003.

[2] T. H. Lin and Y. Y. Sheu, "Theory of laminar flame propagation in near-stoichiometric dilute sprays, Combustion and Flame," Combustion and Flame, pp. 333, 1991.

[3] D. R. Ballal and A. H. Lefebvre, "Flame Propagation in Heterogeneous Mixtures of Fuel Droplets, Fuel Vapor and Air," Proc. Combust. Inst., 1981.

[4] G. D. Myers and A. H. Lefebvre, "Propagation in Heterogeneous Mixtures of Fuel Drops and Air," Combustion and Flame, vol. 66, pp. 193-210, 1986.

[5] G. A. Richards and A. H. Lefebvre, "Turbulent Flame Speeds of Hydrocarbon Fuel Droplets in Air," Combustion and Flame, vol. 78, pp. 299-307, 1989.

[6] D. Bradley, A. K. C. Lau, and M. Lawes, "Flame Stretch Rate as a Determinant of Turbulent Burning Velocity," Phil. Trans. R. Soc. Series A, vol. 338, pp. 359, 1992.

[7] J. T. Farrell, W. Weissman, R. J. Johnston, J. Nishimura, T. Ueda, and Y. Iswashita, "Fuel Effects on SIDI Efficiency and Emissions," SAE 2003-01-3186, 2003.

[8] F. Akamatsu, K. Nakabe, Y. Mizutani, M. Katsuki, and T. Tabata, "Structure of Spark-Ignited Spherical Flames Propagating in a Droplet Cloud," in Developments in Laser Techniques and Applications to Fluid Mechanics, R. J. Adrian, Ed. Berlin: Springer-Verlag, 1996, pp. 212-223.

[9] K. Nakabe, Y. Mizutani, F. Akamatsu, M. Fuchihata, and S. H. ElEmam, "Spark-Ignited Spherical Flames Propagating in a Suspended Droplet Cloud," 5th International Conference on Liquid Atomization and Spray Systems (ICLASS-91), 1991.

[10] Y. Mizutani and A. Nakajima, "Combustion of Fuel Vapour-Drop-Air Systems: Part I, Open Burner Flames," Combustion and Flame, vol. 20, pp. 343-350, 1973.

[11] Y. Mizutani and A. Nakajima, "Combustion of Fuel Vapour-Drop-Air Systems: Part II, Spherical Flames in a Vessel," Combustion and Flame, vol. 21, pp. 351-357, 1973.

[12] G. E. Andrews and D. Bradley, "Determination of Burning Velocities, A Critical Review," Combustion and Flame, vol. 18, pp. 133-153, 1972.

[13] A. Palm-Leis and R. A. Strehlow, "On the Propagation of Turbulent Flames," Combustion and Flame, vol. 13, pp. 111-129, 1969.

[14] M. Z. Haq, "Fundamental Studies of Premixed Combustion," School of Mechanical Engineering, University of Leeds, 1998.

[15] F. Atzler, "Fundamental Studies of Aerosol Combustion," Depart ment of Mechanical Engineering, University of Leeds, 1999.

[16] J. Chomiak, Combustion. A Study in Theory, Fact and Application. New York: Abacus Press/Gordon and Breach Science Publishers, 1990.

[17] G. S. Settles, Schlieren & Shadowgraph Techniques, Berlin: Springer, 2001.

[18] S. Hayashi and S. Kumagai, "Flame Propagation in Fuel Droplet-Vapor-Air Mixtures," Proc. Combustion Institute, 1974.

[19] S. Hayashi, S. Kumagai, and T. Sakai, "Propagation Velocity and Structure of Flames in Droplet-Vapor-Air Mixtures," Combustion Science & Technology, vol.15, pp. 169-177, 1976.

[20] A. S. Mokhtar, "Fundamental Study of Ignition and Combustion of Two Phase Flows at Gas Turbine Conditions," School of Mechanical Engineering, University of Leeds, 2001.

[21] N. Marquez, "Fundamental Studies of Aerosol Flames," School of Mechanical Engineering, University of Leeds, 2003.

[22] G. F. Hundy, "Flame Propagation in a Closed Vessel," School of Mechanical Engineering, University of Leeds, 1969.

[23] D. Bradley, P. H. Gaskell, and X. J. Gu, "Burning Velocities, Markstein Lengths and Flame Quenching for Spherical Methane-Air Flames: A Computational Study," Combustion and Flame, vol. 104, pp. 176-198, 1996.

[24] K. T. Aung, L. K. Tseng, M. A. Ismail, and G. M. Faeth, "Response to Comment by S. C. Taylor abnd D. B. Smith on 'Laminar Burning Velocities and Markstein Numbers of Hydrocarbon/Air Flames'," Combustion and Flame, vol. 109, pp. 526-530, 1995.

[25] D. Bradley, R. A. Hicks, M. Lawes, C. G. W. Sheppard, and R. Woolley, "The Measurement of Laminar Burning Velocities and Markstein Numbers of Iso-Octane-Air and Iso-Octane-n-Heptane-Air Mixtures at Elevated Temperatures and Pressures in an Explosion Bomb," Combustion and Flame, vol. 115, pp. 126-144, 1998.

[26] P. Clavin, "Dynamic Behavious of Premixed Flame Fronts in Laminar and Turbulent Flows," Progress in Energy and Combustion Science, vol. 11, pp. 1-59, 1985.

[27] L. Gillespise, M. Lawes, C. G. W. Sheppard, and R. Woolley, "Aspects of Laminar and Turbulent Burning Velocity Relevant to S.I. Engines," SAE 2000-01-0192, 2000.

[28] X. J. Gu, M. Z. Haq, M. Lawes, and R. Woolley, "Laminar Buring Velocity and Markstein Lengths of Methane Air Mixtures," Combustion and Flame, vol. 121, pp. 41-58, 2000.

[29] E. G. Groff, "The Cellular Nature of Confined Sperical Propane-Air Flames," Combustion and Flame, vol. 48, pp. 51-62, 1982.

[30] S. A. Sulaiman, "Burning Rates and Instabilities in the Combustion of Droplet and Vapour Mixtures," Department of Mechanical Engineering, University of Leeds, 2006.

[31] C. T. R. Wilson, "Condensation of Water Vapour in the Presence of Dust-Free Air and Other Gases," Proc. of the Royal Society of London, 1897.

[32] F. Atzler, M. Lawes, Y. Lee, and S. A. Sulaiman, "Burning Velocities and Instabilities in Centrally Ignited Laminar Flames of Droplet-Vapor-Air Mixtures," in preparation.

[33] R. Woolley, "Personal Communication," 2006.

[34] M. P. Ormsby, "Turbulent Flame Development in a High-Pressure Combustion Vessel," Department of Mechanical Engineering, University of Leeds, 2005.

[35] Y. Ali, D. Bradley, M. Lawes, and E. M. J. Mushi, "Problems of the Measurement of Markstein Lengths with Explosion Flames," The Combustion Institute, Proceedings of the British and German Sections, Queen's College Cambridge, 1993.

PROFILE

ENGR. DR SHAHARIN ANWAR BIN SULAIMAN
Engr. Dr Shaharin Anwar Bin Sulaiman graduated in 1993 with a B.Sc. in Mechnical Engineering from Iowa State University. He earned his M.Sc. in Thermal Power and Fluids Engineering from UMIST in 2000, and Ph.D. in Combustion from the University of Leeds in 2006. During his early years as a graduate, he worked as Mechanical and Electrical (M&E) Project Engineer in Syarikat Pembenaan Yeoh Tiong Lay (YTL) for five years. His research interests include combustion, sprays and atomization, HVAC and renewable energy. He joined Universiti Teknologi PETRONAS (UTP) in 1998 as a tutor, and has become a lecturer in the Mechanical Engineering program since 2000. He is also a certified Professional Engineer with the Board of Engineers, Malaysia, and a Corporate Member of The Institution of Engineers, Malaysia (IEM).